nature climate change

ARTICLES

PUBLISHED ONLINE: 12 FEBRUARY 2012 | DOI: 10.1038/NCLIMATE1410

Global trends in tropical cyclone risk

P. Peduzzi[1,2]*, B. Chatenoux[1,3], H. Dao[1,4], A. De Bono[1,3], C. Herold[1,3], J. Kossin[5], F. Mouton[6] and O. Nordbeck[1]

The impact of tropical cyclones on humans depends on the number of people exposed and their vulnerability, as well as the frequency and intensity of storms. How will the cumulative effects of climate change, demography and vulnerability affect risk? Conventionally, reports assessing tropical cyclone risk trends are based on reported losses, but these figures are biased by improvements to information access. Here we present a new methodology based on thousands of physically observed events and related contextual parameters. We show that mortality risk depends on tropical cyclone intensity, exposure, levels of poverty and governance. Despite the projected reduction in the frequency of tropical cyclones, projected increases in both demographic pressure and tropical cyclone intensity over the next 20 years can be expected to greatly increase the number of people exposed per year and exacerbate disaster risk, despite potential progression in development and governance.

Tropical cyclones (TCs) are common in many regions of the world and affect nearly all tropical areas (Fig. 1). They are associated with extreme winds, torrential rains triggering floods and/or landslides, high waves and damaging storm surges leading to extensive coastal flooding.

Between 1970 and 2009, singular TC events inflicted the highest death toll (Bhola, Bangladesh, 1970, 300,000 killed) and greatest damages (Katrina, USA, 2005, US$125 billion of losses) on record. They claimed a cumulated reported 789,000 lives during this period[1]. Mortality and losses vary extensively from one event to another. Understanding the probability of losses requires an identification of all the components of risk[2,3], which are the hazard (frequency and intensity), the exposure (the number of people; assets or crops) present in the hazard-prone area[4] and the vulnerability (the degree of loss to each element should a hazard of a given severity occur[5]). Given that hazard, exposure and vulnerability are changing, the risk is dynamic and needs to be re-assessed periodically.

Regarding TC hazard, the influence of observed climate change on past TC frequency and intensity is uncertain, and confidence that there have been detectable long-term trends remains low[6]. However, owing to consistency among the models and their agreement with theory, there is greater confidence in twenty-first-century projections of TC activity under warming scenarios. Specifically, whereas it is likely that overall global TC frequency will decrease (or remain roughly constant), it is also likely that mean intensity will increase. Such an increase is expected to be manifest notably in the most intense storms[7] and increases in the frequency of the strongest storms are possible[6,8].

More than the trend in hazards, governments and the insurance industry need information on the trend in mortality and economic risk induced by these hazards. Most global reports looking at trend in disaster risk are based on past reported losses from international databases (mostly from EMDAT; ref. 1).

The number of TC disasters reported by EMDAT has nearly tripled between the 1970s and 2000s (line E in Table 1). Although we cannot discard impacts from climate change on hazard, the improved access to information may be responsible for spurious increases and needs to be assessed.

Carrying out a trend analysis presupposes that such databases are comprehensive or at least consistent through time. However, by comparing observed TC events (as detected by satellite) and reported disasters, there are some large differences in trend. The average observed global TC frequency has remained steady in the past 40 years (line A in Table 1). The number of TCs making landfall, their intensity and the number of countries struck is also stable (lines B, C and D; One TC event can affect several countries. For example, Hurricane Mitch led to disasters in eight different countries and is recorded as eight disasters in EMDAT.). The world population increased by 86% between 1970 and 2010 (ref. 9; from 3.7 to 6.9 billion) and the exposure has therefore increased. However, this has not translated into higher reported mortality, which has fluctuated but is on a downward trend (line F in Table 1).

Therefore, either the increase in exposure was compensated by a significant decrease in vulnerability, and/or the observed increase in reporting is mostly induced by improved access to information. The latter is quite probable given the improvements in global TV coverage, internet, mobile phone and satellite networks[9].

Without undermining the value of international loss databases, these simple statistics show that these are likely to be biased by improvements to technology and information access; they are not comprehensive and they do not indicate whether high losses result from high exposure, high intensity or high vulnerability. Hence, they are not suited for risk trend analysis. Despite these significant limitations, most global reports are based on figures from reported losses[10–14]. A new approach is needed. The method introduced here provides a trend analysis on mortality risk based on the observed TC database[15] further modelled using geographical information system (GIS) and statistical regression. It is independent from international loss databases, which are only used for initial calibrations.

[1]Global Change and Vulnerability Unit, DEWA/GRID-Geneva, United Nations Environment Programme, 11, ch. Anémones, 1219 Châtelaine, Geneva, Switzerland, [2]Institute of Geomatics and Risk Analysis (IGAR), Faculty of GeoSciences and Environment, Amphipôle, University of Lausanne, 1015 Lausanne, Switzerland, [3]Institut F. A. Forel, Faculty of Sciences, University of Geneva, 10, Route de Suisse, 1290 Versoix, Switzerland, [4]Department of Geography, University of Geneva, Faculty of Economic and Social Sciences, Uni Mail, 40, Bd du Pont-d'Arve, 1211 Geneva, Switzerland, [5]National Climatic Data Center/NOAA, 151, Patton Avenue, Asheville, North Carolina 28801-5001, USA, [6]Institut Fourier, University of Grenoble, 100, rue des maths, BP 74, 38402 St Martin d'Hères, France. *e-mail: Pascal.Peduzzi@unepgrid.ch.

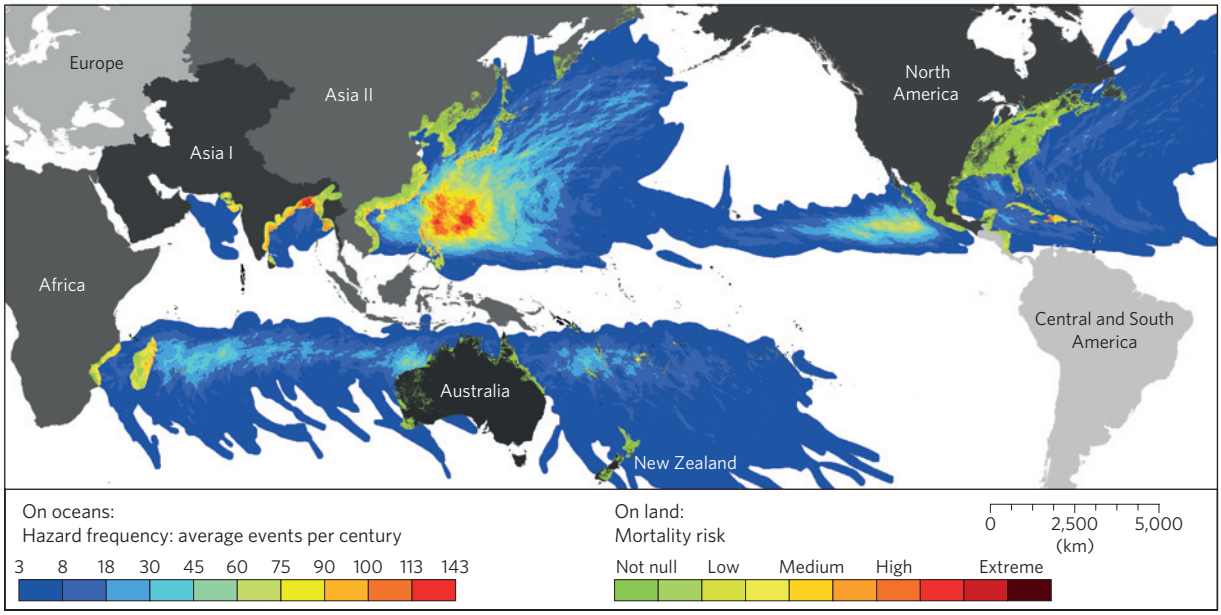

Figure 1 | Map showing distribution of hazard frequency and mortality risk from TCs for the year 2010. Estimates are applied to all pixels on a geographic grid. Mortality risk is categorized from low to extreme.

Table 1 | Events as recorded by instruments (lines A–D) versus trend of reported TC disasters (lines E and F, average per year).

		1970s	1980s	1990s	2000s
A	Number of TC physical events (recorded)[15]	88.4	88.2	87.2	86.5
B	Number of TC events making landfall (recorded)	34.4	34.4	35.6	35.2
C	Weighted average intensity over landfall*	1.7	1.8	1.8	1.8
D	Number of times that TCs hit countries (recorded)	142.1	144.0	155.0	146.3
E	TC disasters in EM-DAT (reported)	21.7	37.5	50.6	63.0
F	Killed (×1,000) by TCs in EM-DAT (reported)	35.7	4.7	21.1	17.4
G	Percentage of reported disasters versus countries hit by TCs	15%	26%	33%	43%

The percentage of reported disasters increased threefold, whereas the number of TCs remained stable. *Weighted average is the sum of all maximum intensity, divided by the number of observed TCs.

Results

The new layers of information produced include TC-hazard global distributions such as average TC frequency, and maximum intensity recorded between 1970 and 2009 as well as total sum of winds. We also provide the TC-exposure distribution (population and gross domestic product (GDP) for each class of intensity) and mortality-risk distribution by class (Fig. 1). These layers of information are made available in different GIS formats. The GIS raster values on exposure and risk were also aggregated (summed) at country level in a tabular format (Supplementary Table S12 in Section S6.3).

The multiple regression analysis showed that the intensity of the hazard, the level of population exposure, the level of poverty and the level of governance were the main factors accounting for risk. It also showed that vulnerability parameters have more weight for less intense TCs and, conversely, the role of population exposure in mortality risk grows with the intensity of the TC. Exposure accounted for 9.0%, 46.4%, 52.7% and 62.9% of mortality losses for TC categories I, II, III and IV respectively (Supplementary Section S6). For category V, human exposure to winds and number of the coastal population living in low-lying areas accounted for 68.9% of the model's losses. However, for this latter category there were too few events for a sound statistical analysis. Poverty levels (low GDP per capita) accounted for 91% of the mortality loss for category I TCs and 37.1% for category IV (and 31.1% for category V). This shows that poverty levels are less significant when facing very intense TCs, whereas at lower intensities only the poorest suffer heavy losses.

Coastal population living in low-lying areas (less than 10 km from the coast) was found to explain a large share of losses from high-category TCs, whereas remoteness was also identified as triggering more vulnerability. According to this analysis, TCs seem to be more dangerous in rural/remote areas as compared with cities. This may be due to several factors, such as improved early warning, better infrastructure, and quicker access to external rescue and aid from humanitarian services in urban areas. Remote locations are more disconnected and less accessible.

The tropical-cyclone mortality-risk index

The mortality risk was aggregated at country level according to two logarithmic scales: average number expected killed per year (absolute risk) and number killed per million inhabitants (relative risk). If absolute risk is employed large countries will rank first, whereas if relative risk is used small islands will appear foremost. To overcome this issue, the two scales were combined to produce 10 categories of countries at risk. This provides a TC mortality-risk index (TC-MRI; Fig. 2). The detailed ranking and categories of countries are provided in Supplementary Table S12 (Supplementary Section S6.3). The TC-MRI provides a standardized tool for comparing countries. The rank is produced by sorting countries by decreasing TC-MRI value, decreasing relative risk and then decreasing absolute risk.

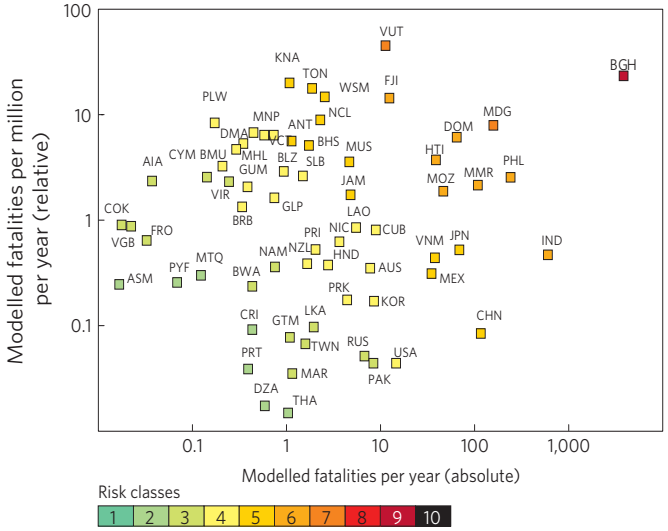

Figure 2 | TC-MRI. The risk categories are based on both average number of people killed per year as modelled (*x* axis) and average number killed per million inhabitants (*y* axis).

As a limitation, the model cannot take mega-disasters (such as Mitch 1998 or Nargis 2008) into account. These are too rare events and thus were statistical outliers in the analysis. The TC-MRI is probably too high for countries that are proactive in disaster risk reduction (DRR) (for example Bangladesh, Japan and Cuba), the reason being that data on DRR (number of shelters, early-warning quality and so on) are not readily available. Comparing TCs Sidr (Bangladesh, 2007) and Nargis (Myanmar, 2008) provides an example of differences from DRR practices. By improving the early-warning system, building shelters and reforesting coastal areas, Bangladesh has succeeded in drastically reducing the number of fatalities related to TCs (ref. 16). Despite the fact that Sidr hit a larger population with stronger winds, it resulted in 30 times fewer victims in Bangladesh than did Nargis in Myanmar[1]. Myanmar's official warning to the population was provided on page 15 of the newspaper *The New Light of Myanmar*[17], suggesting that officials did not take the threat seriously. Bangladesh has drastically reduced the mortality risk, but risk remains high owing to high exposure and poverty levels.

Also, the historical global TC records suffer from well-known heterogeneities due to improvements of methodologies and instruments for measuring TCs. Estimates of TC maximum winds are particularly sensitive to these improvements[18]. This sensitivity can influence the size of the buffers considered in this study and result in a spuriously inflated trend in exposure. To minimize this effect, only the events from 1978 and onward were taken for the event analysis. The results based on TC frequency are less sensitive to data heterogeneity, given the smoothing function applied. The full range of data since 1970 was used to cover as many TC-prone areas as possible. A smaller sample of records would have resulted in an underestimation of the TC-prone areas and associated frequencies.

Mortality-risk trend analysis (1970–2010)

A given population living in a hazard-prone area is not impacted every year by hazardous events. The average number of people exposed annually to hazards is called 'physical exposure' and mathematically can be obtained by multiplying the number of people living in the hazard-prone area by the annual frequency of occurrence of a selected hazard.

In 2010, an estimated 1.53 billion people were living in TC-prone areas in 81 different countries and territories. The average yearly number of people exposed to TCs is estimated at 133.7 million. An average of US$1,901 billion is exposed annually to TCs, out of the 16,281 billion located in TC-prone areas. Computing trends in physical exposure requires information on both hazard frequencies and demographic changes (Supplementary Section S6).

In the model, values of exposure and vulnerability were replaced by values for the specific years (1970, 1980, 1990, 2000 and 2010) and used to identify trends based on vulnerability and exposure while holding hazard constant. This enables removal of the effect of seasonal variations.

At constant hazard, risk is a product of exposure and vulnerability. In Fig. 3, the *y* axis is the vulnerability (expressed as number killed per million exposed). The *x* axis is the number of people exposed (in millions). The multiplication of vulnerability by exposure provides the risk. Each point in Fig. 3 is the top right corner of a rectangle whose area is equal to the level of risk. In this way it is possible to see if the risk is triggered more by exposure or by vulnerability. The dashed lines represent the equirisk levels, where, for example, the increase in exposure is exactly compensated by corresponding decrease in vulnerability in such a way that risk remains unchanged. This is the case for North America, where despite a 58% increase in exposure between 1970 and 2010 the risk remained constant owing to a corresponding decline in vulnerability. All regions have an increasing exposure due to demographic pressure, but some regions manage to reduce their risk despite an increase in exposure. For example, in Asia

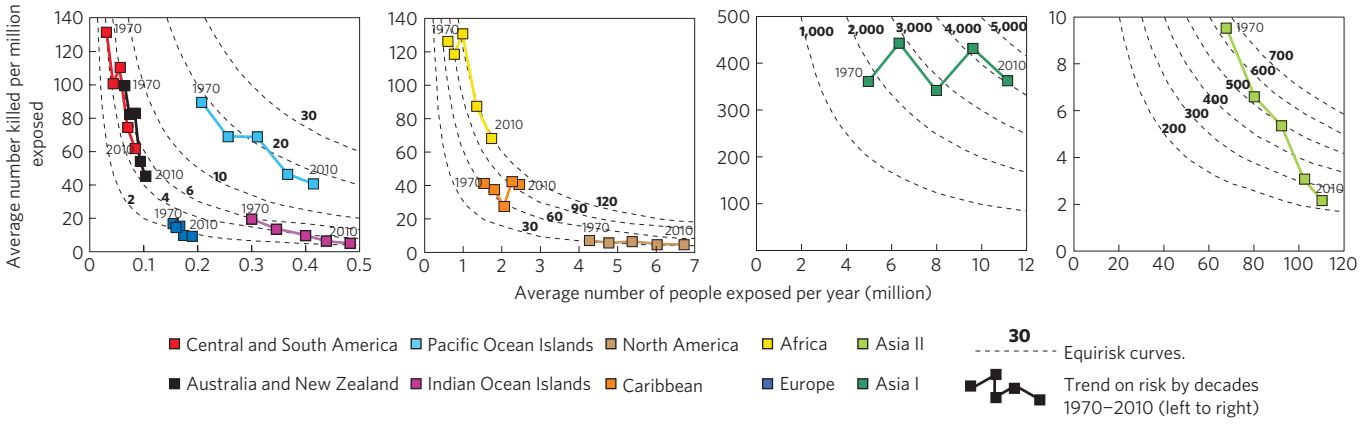

Figure 3 | Trends in TC exposure, vulnerability and risk by Intergovernmental Panel on Climate Change regions from 1970 to 2010. The *y* axis represents the vulnerability (in number killed per million exposed); the *x* axis represents the number exposed (in million). The area of the virtual rectangles where the bottom left corner is the origin (0, 0) and each coloured square is the top right corner is equal to the level of risk. The dashed lines represent equirisk levels.

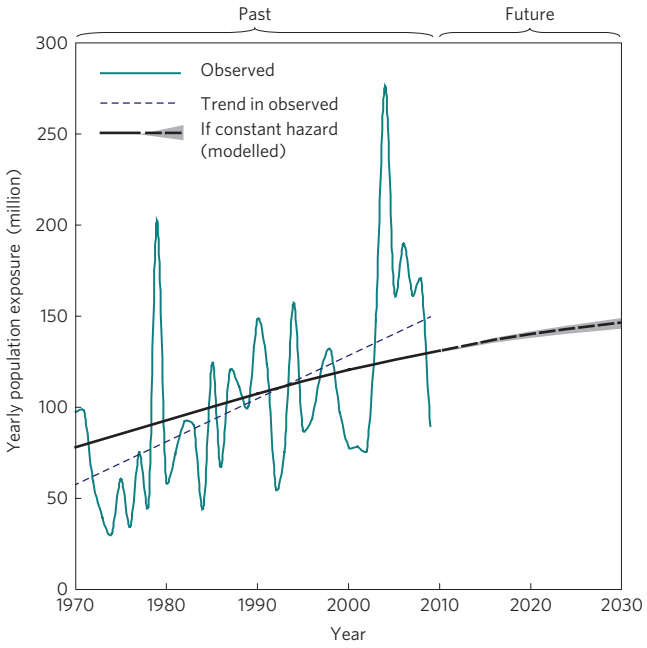

Figure 4 | Change in TC population yearly exposure with time. For the period 1970–2009 the exposure is provided for both observed and average trend (assuming constant hazard). The period 2010–2030 includes only the average trend under constant hazard, with uncertainty from population growth (−2.2 to 1.0%).

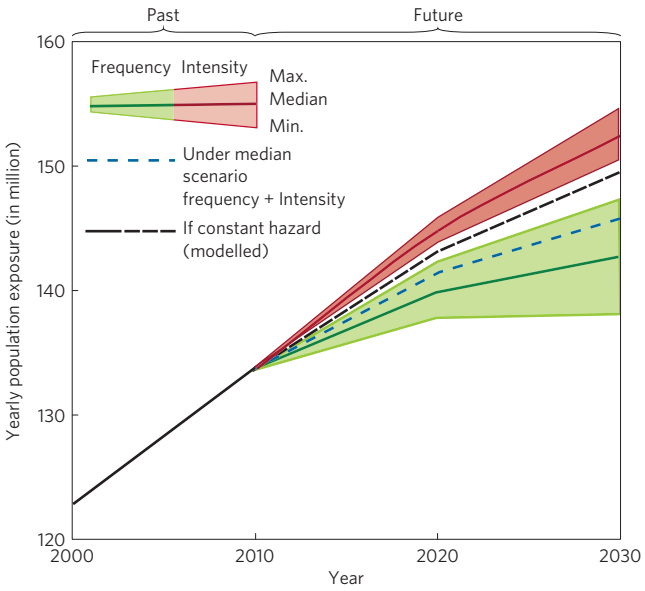

Figure 5 | Scenarios until 2030. Influence of hazard on exposure for increase in intensity (red) and change (decrease) in frequency (green) and median scenario (dashed line in blue).

II (Asian countries on the Pacific Ocean, Fig. 1), the level of risk was reduced by 300% owing to a drastic reduction in vulnerability (that is more than 70% reduction since 1970). The trend in this region is largely influenced by China. In Asia I (India, Bangladesh and Myanmar), the vulnerability remains very high and fluctuates around 400 killed per million exposed. Progress in DRR has been made in Bangladesh (for example, number of shelters built). However, such indicators were not available globally for inclusion in the models. Both the exposure and risk have more than doubled in this region since 1970.

Scenarios for 2030

The United Nation projection for world population in 2030 is 8.3 billion people[19] (8.2–8.5; ref. 20). This change in demography will influence the exposure to hazards. Since 2010, more than 50% of the population has been urban. Our study reveals that urban population is usually less vulnerable to TC hazards. However, about a third of the urban population live in slums, and such a habitat often does not provide safe haven when compared with areas with better construction. Instead of providing shelter, the construction material can actually escalate the risk (for example flying corrugated roofing material). The population in the slums is also often from inland rural areas and may be less prepared for and informed about TCs.

In Fig. 4, yearly exposure depends on several factors, the main parameters being the number of intersections of TC events with land, the population density at the affected locations and the size of the TC footprint. The observed exposure reveals high variability. However, the trend follows the theoretical average exposure (assuming constant hazard), although the average trend in observed exposure is steeper than the modelled trend (which suggests either a change in hazard or influence in instrument and/or method improvements). For the extrapolation to 2010–2030, only the average exposure is provided (Fig. 4).

Assuming constant hazard, the population growth would increase the average population exposed per year to 149.3 million (+11.7%) by 2030. In relative terms, the main percentage increase in physical exposure to TCs will be in Africa, with +54% (mostly Madagascar and Mozambique). In absolute terms, about 90% of exposure to TCs will occur in Asia. This region will face the highest increase of annual exposure, with +10.7 million for Pacific Asia and +2.5 million for Indian Ocean Asia (see Supplementary Table S6).

According to ref. 6, owing to climate change, global TC frequency is likely to decrease or remain essentially unchanged (−6 to −34% by year 2100), whereas some increase in the mean maximum wind speed of TCs is likely (+2 to +11% globally). Although it is understood that climate and TC activity exhibit substantial natural variability on a range of timescales, here we assume constant linear trends for illustration purposes, and to explore how exposure may change according to summaries of current global TC projections from ref. 6. Under this assumption, the projections of ref. 6 translate to a −1.3 to −7.6% change in frequency and between +0.4 and +2.4% change in intensity by 2030. Figure 5 shows the influence of these changes in hazard frequency and intensity on human exposure.

The influence of frequency on exposure is linear. Following the projections of ref. 6, the potential range of exposure from frequency change would be between 135.5 and 144.6 million people per year (median: 140.1 million) exposed by 2030. The effect of increasing intensity is harder to estimate as more intense TCs often have bigger footprints, thus further compounding the increases in exposure. Also to be taken into account is the possibility for a higher rate of population increase in coastal areas.

Despite uncertainties about these values on the future evolution of TC, we show that, independently from the scenarios, there will be an increase in exposure to TCs triggered mainly by population growth. This is a global trend, and the regional trends include much higher variations (Supplementary Section S7), but also with less confidence in the projections. Even under the most optimistic scenario (7.6% decrease in TC frequency and no increase in TC intensity) on climate change influences on TC, changes in human exposure will increase exposure to TC.

Conclusions

This method proved to be successful in identifying underlying factors of risk, where poverty, governance, intensity and exposure

seem to be the main explanatory variables. The modelling of TC footprints allows for a refined measure of exposure and modelled of average exposure.

In future research, the model used here could be improved. Parameterization of the TC wind field with the Holland[21] model can suffer from inaccuracies and tends to overestimate the area of strong winds[22–24], although there is no expectation that these will project strongly on the trends shown here (see discussion in Supplementary Section S1.3).

Another improvement could be made by using subnational values for vulnerability indicators. The use of national values, especially for large countries such as India and China, does not reflect the significant variations within the countries.

The demographic pressure and the development of new infrastructure will increase the exposure in the coming decades. Regardless of uncertainties in TC projections, the likelihood of increased risk and human exposure suggests that the principle of caution should be observed and should galvanize governments to action.

So far, the reduction in vulnerability has compensated the increase in exposure. If projections of TC-intensity increases are confirmed, the outcome could be different because exposure trends tend to increase at higher intensities, as exposure plays a heavier role with high-intensity TCs. Further investigations include continuing research on the impacts of climate change on the intensity of TCs as well as introducing these impacts into the footprints and risk models.

Methods

Modelling TC wind fields and tracks using mathematical formulas associated with GIS techniques is a well-recognized approach[25,26]. Characterization of the hazard is generally based on linear interpolation through Monte Carlo simulation of best tracks (or synthetic tracks) for computing probability of occurrence of wind-speed hazards[27–31]. Surfaces covered by TCs are usually modelled either through kernel smoothing of best tracks[29] or the creation of circular buffers derived from the maximum sustained wind speed[32], but mathematical models based on central pressure and maximum wind speed provide more realistic results. The Holland model[21], and its derivatives, is probably the most used and recognized hurricane hazard model, despite a known tendency to overestimate the radius of maximum wind[22–24]. It produces wind-speed profiles for a specific time[26]. We transformed this model to produce TC wind-speed surfaces over time.

Most studies including hazards and change in exposure have mostly focused on small areas[25,27] or one country[32]. Risk analyses have mainly focused on economic losses[25,27,33]. None of the aforementioned studies attempt to cover the whole world.

We provide here results from 3D modelling (wind-speed profile footprints through time) of all individual TC events available (4,182) from 1970 to 2009 for the entire globe. We intersected these modelled surfaces of wind intensities with models of human and economic distribution (at a resolution of 30 arc second) for the corresponding years to compute the exposures under each hazardous event footprint. We then linked these footprints with reported losses (killed and economic losses) using a previously developed methodology (ref. 34), as well as contextual vulnerability parameters using indicators of economy, development level, governance, political corruption, quality of environment and demography, as well as remoteness, proximity from the coast and other parameters (Supplementary Table S3). To this end, we compiled a vulnerability database with 124,000 records on about 40 indicators for 40 years and 208 countries and territories. Some indicators were not available and data gaps remain a limitation for selected indicators. Exposure and vulnerability parameters were used to infer the loss functions using statistical multiple regressions. This provides the TC hazard distribution for the five different Saffir–Simpson intensity classes, the distribution of human and economic exposure, an identification of the vulnerability parameters which are associated with TC risk and a quantitative evaluation of the role of exposure and vulnerability in configuring risk. The risk was mapped to show its geographic distribution and values were aggregated at the national level to compare countries. We also replaced original values of exposure and vulnerability for the corresponding values of 1970, 1980, 1990, 2000 and 2010 to identify the trend in risk. Finally, values of exposure were extrapolated for year 2030 to evaluate the respective influences of both climate change and population growth on future human exposure to TCs.

The method follows an eight-step process (see Supplementary Section S1 for details), starting from hazard modelling, evaluation of human and economic exposure (using the LandScan population model[35] and a GDP distribution model) and identification of contextual vulnerability parameters from a list of about 40 parameters. It enables the creation of an MRI to compare countries.

Received 28 October 2011; accepted 10 January 2012; published online 12 February 2012

References

1. EM-DAT: The OFDA/CRED International Disaster Database http://www.emdat.be (2011).
2. Tobin, G. A. & Montz, B. E. *Natural Hazards: Explanation and Integration* (Guilford Press, 1997).
3. United Nations Disaster Relief Coordinator *Natural Disasters and Vulnerability Analysis in Report of Expert Group Meeting* 8–9 (UNDRO, 1979).
4. http://www.preventionweb.net/english/professional/terminology/?pid:6&pih:2.
5. Coburn, A. W., Spence, R. J. S. & Pomonis, A. Vulnerability and risk assessment. *UNDP Disaster Management Training Program* Vol. 57 (1997).
6. Knutson, T. R. *et al.* Tropical cyclones and climate change. *Nature Geosci.* **3,** 157–163 (2010).
7. Elsner, J. B., Kossin, J. P. & Jagger, T. H. The increasing intensity of the strongest tropical cyclones. *Nature* **455,** 92–95 (2008).
8. Bender, M. A. *et al.* Modeled impact of anthropogenic warming on the frequency of intense Atlantic hurricanes. *Science* **327,** 454–458 (2010).
9. Peduzzi, P., Dao, H., Herold, C. & Mouton, F. Assessing global exposure and vulnerability towards natural hazards: The Disaster Risk Index. *Nat. Hazard. Earth Syst. Sci.* **9,** 1149–1159 (2009).
10. World Bank *Development Actions and the Rising Incidence of Disasters, Evaluation Brief #4* (Independent Evaluation Group, the World Bank, 2007).
11. ESCAP, UNISDR *Protecting Development Gains, Reducing Disaster Vulnerability and Building Resilience in Asia and the Pacific* (ESCAP, UNISDR, 2010).
12. IFRC *World Disasters Report: Focus on Early Warning, Early Action* (IFRC, 2009).
13. ICHARM, UNESCO *Global Trends in Water-Related Disasters: An Insight for Policymakers* (ICHARM, UNESCO, 2009).
14. DARA *Climate Vulnerability Monitor 2010: The State of the Climate Crisis* (Development Assistance Research Associates (DARA), 2010).
15. Knapp, K. R., Kruk, M. C., Levinson, D. H., Diamond, H. J. & Neumann, C. J. The International Best Track Archive for Climate Stewardship (IBTrACS): Unifying tropical cyclone best track data. *Bull. Am. Meteorol. Soc.* **91,** 363–376 (2010).
16. Paul, B. K. Why relatively fewer people died? The case of Bangladesh's Cyclone Sidr. *Nat. Hazard.* **50,** 289–304 (2009).
17. Webster, P. J. Myanmar's deadly daffodil. *Nature Geosci.* **1,** 488–490 (2008).
18. Landsea, C. W., Harper, B. A., Hoarau, K. & Kaff, J. Can we detect trends in extreme tropical cyclones? *Science* **313,** 452–454 (2006).
19. United Nations Population Division, Population 1960–2010 http://geodata.grid.unep.ch/.
20. Raftery, A. E. *et al. White Paper: Probabilistic Projections of the Total Fertility Rate for all Countries for the 2010 World Population Prospects* (2009); available at http://www.un.org/esa/population/meetings/EGM-Fertility2009/P16_Raftery.pdf.
21. Holland, G. J. An analytic model of the wind and pressure profiles in hurricanes. *Mon. Weath. Rev.* **108,** 1212–1218 (1980).
22. Willoughby, H. E. & Rahn, M. E. Parametric representation of the primary hurricane vortex. Part I: Observations and evaluation of the Holland (1980) model. *Mon. Weath. Rev.* **132,** 3033–3048 (2004).
23. Willoughby, H. E., Rahn, M. E. & Darling, R. W. R. Parametric representation of the primary hurricane vortex. Part II: A new family of sectionally continuous profiles. *Mon. Weath. Rev.* **134,** 1102–1120 (2006).
24. Holland, G. A revised hurricane pressure–wind model. *Mon. Weath. Rev.* **136,** 3432–3445 (2008).
25. Davidson, R., Zhao, H. & Kumar, V. Quantitative model to forecast changes in hurricane vulnerability of regional building inventory. *J. Infrastruct. Syst.* **9,** 55–64 (2003).
26. Vickery, P. J., Skerlj, P. F., Steckley, A. C. & Twisdale, L. A. Hurricane wind field model for use in hurricane simulations. *J. Struct. Eng.* **126,** 1203–1221 (2000).
27. Jain, V. K., Davidson, R. & Rosowsky, D. Modelling changes in hurricane risk over time. *Nat. Hazard. Rev.* **6,** 88–96 (2005).
28. Apivatanagul, P., Davidson, R., Blanton, B. & Nozick, L. Long-term regional hurricane hazard analysis for wind and storm surge. *Coast. Eng.* **58,** 499–509 (2011).
29. Poulos, H. M. Spatially explicit mapping of hurricane risk in New England, USA using ArcGIS. *Nat. Hazard.* **54,** 1015–1023 (2010).
30. Rumpf, J., Weindl, H., Höppe, P., Rauch, E. & Schmidt, V. Tropical cyclone hazard assessment using model-based track simulation. *Nat. Hazard.* **48,** 383–398 (2008).
31. Legg, M. R., Nozick, L. K. & Davidson, R. A. Optimizing the selection of hazard-consistent probabilistic scenarios for long-term regional hurricane loss estimation. *Struct. Safety* **32,** 90–100 (2010).
32. Esteban, M. & Longarte-Galnares, G. Evaluation of the productivity decrease risk due to a future increase in tropical cyclone intensity in Japan. *Risk Anal.* **30,** 1789–1802 (2010).

33. Vickery, P. J., Masters, F. J., Powell, M. D. & Wadhera, D. Hurricane hazard modelling: The past, present, and future. *J. Wind Eng. Ind. Aerodyn.* **97,** 392–405 (2009).
34. Peduzzi, P., Dao, H. & Herold, C. Mapping disastrous natural hazards using global datasets. *Nat. Hazard.* **35,** 265–289 (2005).
35. Landscan, Oak Ridge National Laboratory, http://www.ornl.gov/sci/landscan/.

Acknowledgements

U. Deichmann (World Bank) for providing the GDP distribution; A. Maskrey (United Nations International Strategy for Disaster Reduction) for finding the finances to supporting this study; R. Harding for English corrections.

Author contributions

P.P. developed the methodology, carried out the multiple-regression risk analysis, including trend and spatial risk distribution, and developed the MRI with H.D. B.C., C.H. and O.N. generated the spatial model for the TC buffers and extracted the human and economic exposure as well as contextual parameters. F.M. did the mathematical models for the TC buffers. H.D. produced the model of population distribution for 1970–2030 and produced the database on socio-economic parameters. A.D.B. georeferenced the losses and estimated the coastal population living in low-lying areas. J.K. and P.P. developed the method for extrapolating exposure and frequency for 2030 on the basis of a review of different climate change scenarios. P.P. is the lead author, with advice and critical review from J.K. and key contributions from all co-authors.

Additional information

The authors declare no competing financial interests. Supplementary information accompanies this paper on www.nature.com/natureclimatechange. Reprints and permissions information is available online at www.nature.com/reprints. Correspondence and requests for materials should be addressed to P.P.